Available online at www.sciencedirect.com
SCIENCE DIRECT®
Journal of Computational Physics 214 (2006) 491–504
JOURNAL OF COMPUTATIONAL PHYSICS
www.elsevier.com/locate/jcp

Modelling multi-viscosity systems with dissipative particle dynamics

D.C. Visser *, H.C.J. Hoefsloot, P.D. Iedema

Faculty of Science, University of Amsterdam, Nieuwe Achtergracht 166, 1018 WV, Amsterdam, The Netherlands

Received 23 December 2004; received in revised form 14 September 2005; accepted 28 September 2005
Available online 10 November 2005

Abstract

Dissipative particle dynamics (DPD) is a particle-based simulation technique. It is applicable on time and length scales in-between those typical for molecular modelling and continuum mechanics. These features make DPD an interesting tool in the area of multiphase flows. So far, multiphase DPD simulations were restricted to fluids with the same viscosity, because it was unclear how one could model phases with a different viscosity together. Here, we show how to deal with more than one viscosity in the system. The viscosity of a DPD fluid can be controlled with the friction factor, an input parameter in DPD that characterises the strength of the drag force between interacting particles. So, in a multiphase system each fluid has its own friction factor, yielding the viscosity of that fluid. Now, the problem is to define the friction factor for the interaction between particles of unlike fluids. This factor has a significant effect on flow dynamics, but lacks a related physical property such as interfacial tension or solubility to specify its value. Three methods are presented to calculate the friction factor between particles of unlike fluids. One of these methods only involves the friction factors of the individual fluids and is of most practical use in real applications. The methods are validated for steady and unsteady flow of two adjacent immiscible fluids. Results from these two-phase test cases are consistent with theory. This opens the door to more extensive modelling of multi-viscosity systems with DPD.

Keywords: Dissipative particle dynamics; Multiphase flow; Viscosity; Interface

1. Introduction

Microscopic phenomena play a key role in the dynamic behaviour of multiphase systems. The molecular conformation affects, for instance, the miscibility and interface dynamics of species. Breakup and coalescence of fluid portions involve pressure gradients and flow on a scale equal to the thickness of the interface. The macroscopic description of conventional continuum-based simulation techniques is often insufficient to model such complex microscopic processes. On the other hand, detailed molecular modelling of multiphase

* Corresponding author. Tel.: +31 20 525 5265; fax: +31 20 525 5604.
E-mail addresses: visser@science.uva.nl (D.C. Visser), piet@science.uva.nl (P.D. Iedema).

0021-9991/$ - see front matter © 2005 Elsevier Inc. All rights reserved.
doi:10.1016/j.jcp.2005.09.022

flow is computationally too intensive. Simulation techniques applicable between a microscopic and macroscopic scale are, therefore, particularly useful in this area. A particle-based form of such a mesoscopic technique is dissipative particle dynamics or DPD. Initially this coarse grained approach was introduced by Hoogerbrugge and Koelman [1] to study colloidal suspensions [2]. Meanwhile, it has been employed in many other problems involving polymers [3–5], phase separation [6,7], interface dynamics [8] and membranes [9].

DPD applied to multiphase systems is mainly concerned with phase separation and interfacial processes with phases that repel each other. To our knowledge, no publications exist on systems containing phases of different viscosity. In real multiphase systems the phases differ in viscosity. Apart from that, viscosity and differences in viscosity between one fluid and another have a strong influence on the dynamic behaviour. It has distinct practical implications, for instance, on the mixing behaviour of fluids. The ability to deal with viscosity differences is therefore essential for realistic modelling of such systems. The viscosity of a DPD fluid can be controlled by increasing or decreasing the drag force between interacting particles. The desired viscosity of a fluid is, thus, associated to a specific drag interaction between the particles of that fluid. However, the fluids in a multiphase system do not only interact with themselves but also with one another. How to define the drag force for this kind of interactions is, as yet, an unresolved issue.

In this paper we study the effect of the drag between unlike fluids in a multiphase system. We show that the choice of this drag force is not arbitrary, since its large impact on flow dynamics. Three different methods are presented to define an appropriate drag interaction between unlike fluids. The first method is an exact one derived from a solution of the flow profile, and is, thus, of little practical use. The second is an approximation based on the assumption that the velocity gradient is constant near the interface. It requires the, often difficult to determine, position of the interface. The third, and most simple, method depends on input parameters alone. Computer experiments show that this last method works just as well as the other two and is, therefore, preferred in real applications.

2. Dissipative particle dynamics algorithm

In the DPD method, the system under consideration is represented by a set of interacting particles. A DPD particle is interpreted as a small fluid package that represent the collective dynamic behaviour of the molecules it contains. The basis of the method consists of calculating and updating the positions and impulses of all particles over time. This is done according Newton's second law of motion and using the modified velocity-Verlet algorithm as presented by Groot and Warren [7]. The force two particles i and j exert on each other is pairwise additive and consists of a dissipative ($\mathbf{F}_{ij}^{\mathrm{D}}$), a random ($\mathbf{F}_{ij}^{\mathrm{R}}$) and a conservative part ($\mathbf{F}_{ij}^{\mathrm{C}}$)

$$\mathbf{f}_{ij} = \mathbf{F}_{ij}^{\mathrm{D}} + \mathbf{F}_{ij}^{\mathrm{R}} + \mathbf{F}_{ij}^{\mathrm{C}}. \tag{1}$$

The total force acting on a particle i is the sum of all $\mathbf{f}_{ij}$ forces it experiences from particles within a certain cut-off radius r_{c}. Here, r_{c} is set to 1 and taken as unit of length. Body forces are imposed simply by adding it as an extra force to each individual particle.

The dissipative or drag force acts as a resistance against relative motion and depends on the velocity difference between particles. This force is, therefore, closely related to the viscosity of the fluid. Eq. (2) gives the mathematical expression for this force, where $r_{ij} = |\mathbf{r}_i - \mathbf{r}_j|$, $\hat{\mathbf{r}}_{ij} = (\mathbf{r}_i - \mathbf{r}_j)/r_{ij}$ and $\mathbf{v}_{ij} = \mathbf{v}_i - \mathbf{v}_j$. The strength of the drag force is determined by the friction factor γ

$$\mathbf{F}_{ij}^{\mathrm{D}} = -\gamma\omega^{\mathrm{D}}(r_{ij})(\hat{\mathbf{r}}_{ij}\cdot\mathbf{v}_{ij})\hat{\mathbf{r}}_{ij}. \tag{2}$$

The random force introduces the Brownian-like, fluctuating character of molecules and is given by Eq. (3), where the factor σ represents the fluctuation amplitude and ζ_{ij} is a random number drawn from a uniform distribution with zero mean and Δt^{-1} variance, where Δt is the time step in the simulation

$$\mathbf{F}_{ij}^{\mathrm{R}} = \sigma\zeta_{ij}\omega^{\mathrm{R}}(r_{ij})\hat{\mathbf{r}}_{ij}. \tag{3}$$

The conservative force is a soft repulsive force representing the effective potential between the particles. The expression for this force is given by Eq. (4), where the repulsion factor a_{ij} is the maximum repulsion between a pair of interacting particles

$$\mathbf{F}_{ij}^{\mathrm{C}} = a_{ij}\omega^{\mathrm{C}}(r_{ij})\hat{\mathbf{r}}_{ij}. \tag{4}$$

The ω's appearing in all three forces are weight functions that take into account the dependency on the interaction distance between particles. These weight functions go to zero when r_{ij} approaches the cut-off radius r_c. Español and Warren [10] showed that the correct thermostat is obtained when the following *fluctuation–dissipation* theorem is satisfied:

$$\omega^{\mathrm{D}}(r_{ij}) = [\omega^{\mathrm{R}}(r_{ij})]^2, \quad k_{\mathrm{B}}T = m\sigma^2/2\gamma, \tag{5}$$

where $k_{\mathrm{B}}T$ is the temperature in the system and m the particle mass. Simulations in this paper are performed in an isothermal system with $m = 1$ for all particles and weight functions $\omega^{\mathrm{R}} = \omega^{\mathrm{C}} = (1 - r_{ij}/r_c)$ [7].

3. Viscosity of a DPD fluid

The transport properties of a DPD fluid cannot be set as input parameters themselves, but instead they follow as measurable quantities resulting from a chosen set of DPD input parameters. Expressing these properties in terms of the input parameters beforehand has been the topic of several DPD studies [1,2,7,11]. Marsh et al. [11] were able to derive a relation for the viscosity, depending on the input parameters temperature $k_{\mathrm{B}}T$, number density n, particle mass m, friction factor γ and cut-off radius r_c. In our case (r_c and m equal to 1) their relation reads as follows:

$$\mu = \frac{45k_{\mathrm{B}}T}{4\pi\gamma} + \frac{2\pi n^2\gamma}{1575}, \tag{6}$$

where the first part is the kinetic contribution μ_{K} to the viscosity, related to particle diffusion, and the second part is the dissipative contribution μ_{D}, related to the friction between particles. In this relation, the contribution from the conservative forces is not taken into account. Although some discrepancy may exist between this theoretical prediction and simulations [11–14], it shows qualitatively how the viscosity depends on the different input parameters.

The friction factor γ in Eq. (6) is a suitable input parameter to control the viscosity of a DPD fluid. In a system of a certain density and temperature, for example, one can tune the viscosity to the desired value by adjusting the friction factor. This is demonstrated in Fig. 1(a), where the viscosity predicted with Eq. (6) is plotted against the friction factor for a system of $n = 10$ at different temperatures. For low values of the friction factor the viscosity is largely determined by the kinetic part in Eq. (6). At higher values of the friction factor the kinetic contribution diminishes and the dissipative part in Eq. (6) starts to dominate the viscosity, as shown in Fig. 1(b). Here, we want to explore this last parameter region where $\mu_{\mathrm{D}} > \mu_{\mathrm{K}}$, a region which

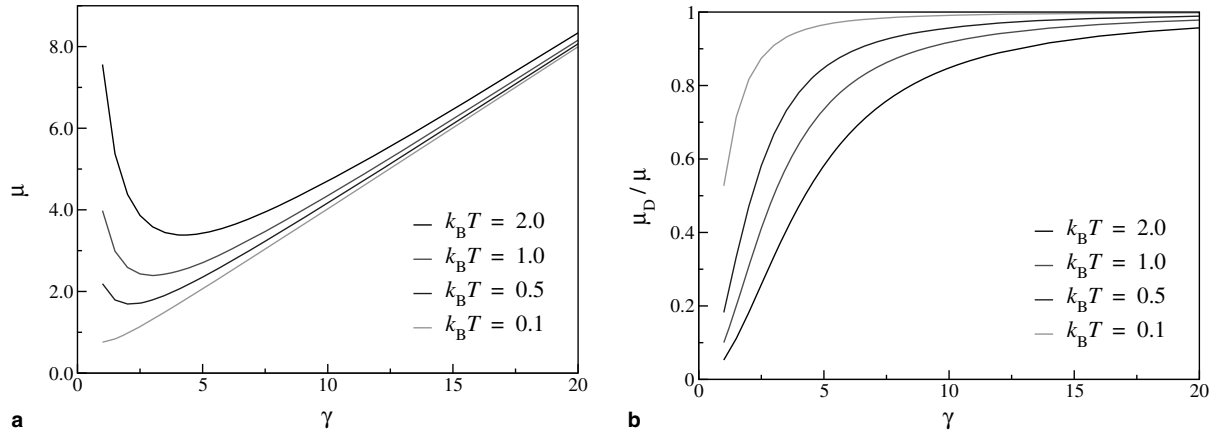

Fig. 1. The dynamic viscosity of a DPD fluid (a) and its dissipative portion (b) as a function of friction factor according Marsh et al. [11] for a systems of $n = 10$ at different temperatures.

previously has been identified as the liquid-like or collective dynamic regime [15,16]. According to Marsh et al. the viscosity scales linearly with the friction factor in this region.

4. Multiple viscosities in DPD

If the fluids in a multiphase system differ in viscosity one friction factor no longer suffices. Then, each fluid has its own specific drag behaviour and a friction factor γ_{ij} must be defined for all different types of interactions separately, that is, interactions between particles i and j of like and unlike fluids. In a comparable way the repulsion factor a_{ij} is specified for the interaction between different species in a multiphase system (see for instance [6,7]). Then, the repulsion between particles of the same fluid determines the compressibility of that fluid and the repulsion between particles of different fluids sets their interfacial tension. Note besides, that through the fluctuation–dissipation theorem in Eq. (5) each friction factor γ_{ij} automatically leads to the definition of a corresponding fluctuation amplitude σ_{ij}.

In a two-phase system of fluid A and B it is obvious that the friction factor for the interaction between particles of type A (γ_{AA}) determines the viscosity of fluid A. The same is true for the friction factor between particles of fluid B (γ_{BB}) and its viscosity. However, the physical interpretation of the drag between particles of different fluids is less obvious, which makes it more difficult to specify the friction factor γ_{AB} for the interaction between type A and B particles. The friction between unlike fluids will probably affect the viscosity as well, but to which extent or scale is a priori unknown. In order to study the effect of this unlike friction factor we model the adjacent flow of two immiscible Newtonian fluids driven by a body force. Here, we follow the idea described in [17] to model Poiseuille flow with periodic boundary conditions. The body force in the adjacent fluid layers points in opposite direction and generates a steady flow with zero velocity on the interfaces. The analytical solution of the velocity profile is known for this stationary *periodic* Poiseuille flow [18] and will serve as a bench mark in our study. Before we present our results we give an overview of the computational details.

4.1. Computational details

The periodic Poiseuille flow simulations are performed with a set of 4800 particles in a rectangular box of sizes $8 \times 10 \times 6$ ($n = 10$) and $k_B T = 0.5$. Half of the particles are of fluid type A and half of fluid type B. The friction factor γ_{AA} is set to 9.0, which gives fluid A a dynamic viscosity of 3.63 ± 0.02. A 10 times higher viscosity is obtained for fluid B when γ_{BB} is set to 109.2. Both viscosities are measured from a single-phase periodic Poiseuille flow simulation [17]. Note, here, that the viscosity does not scale exactly linearly with the friction factor. This is caused by the kinetic contribution to the viscosity, which is still relatively high for fluid A. In reality it is even higher than predicted by Eq. (6). The fluids are placed next to each other by filling the left half of the box with the particles of type A and the right half with the particles of type B.

Periodic Poiseuille flow is induced by imposing a body force $\mathbf{f}_A^b$ on fluid layer A in the positive z-direction and a body force $\mathbf{f}_B^b$ on fluid layer B in the negative z-direction. It forces the fluids in opposite direction and allows periodic boundaries in all directions as shown in [17]. A steady flow with zero velocity on the interfaces will develop when the absolute force on fluid layer A and B is equal, i.e. the net force on the system is zero. Expressing the mass of a layer in terms of density times volume this condition is met when

$$-\frac{\mathbf{f}_A^b}{\mathbf{f}_B^b} = \frac{W_B}{W_A}, \tag{7}$$

where W_A is the width of fluid layer A and W_B the width of fluid layer B. Note that the terms for density, height and depth drop out of the equation, since they are the same for both layers. When Eq. (7) holds the analytical solution of the stationary velocity profile V_z in each layer is given by [18]

$$\phi = 1 - \xi^2 \tag{8}$$

written in the dimensionless variables

$$\phi = \frac{8\mu V_z}{n\mathbf{f}^b W^2}, \quad \xi = \frac{2x - W}{W}, \tag{9}$$

where μ is the dynamic viscosity, $\mathbf{f}^{b}$ the body force and x the position in the layer of width W. In the present situation $W_A = W_B = 4$ and we set the magnitude of the body force on fluid layer A to 9.075×10^{-2}. Then, the body force on fluid layer B follows from Eq. (7) as -9.075×10^{-2}. According to Eq. (8) these settings lead to a maximum absolute velocity $V_z^{\max}$ of 0.5 in the system. The time step Δt is chosen such that $\Delta t \leqslant 0.1/\gamma$, which keeps the drift of the equilibrium temperature within 2% [19]. The simulated stationary velocity profiles are determined after steady-state is reached. They are obtained by dividing the system in 40 slabs and averaging the velocity in each slab over a time span of 200.

Two interfaces are present in the x-direction, one in the middle of the simulation box and one on the periodic boundary. If simple fluids without interfacial tension are used, the DPD model is nothing more than a particle-based (macroscopic) flow solver that obeys the Navier–Stokes equations [1]. In such an ideal situation the simulated velocity profile should, thus, correspond to Eq. (8), which enables verification of the results. Besides, when tension effects at the interface are absent it is possible to study the sole effect of the friction factor on flow dynamics. Both, evidently, very useful characteristics in the present study. To avoid tension effects we define a single repulsion factor in the system, equal for all type of interactions. Here, we use a repulsion factor of $a = 75k_BT/n$, approximately yielding the compressibility of water [7]. A consequence of this uniform repulsion is that fluid A and B are completely miscible, which will frustrate the intended nature of our two-phase flow problem. Therefore, particles that cross the interface undergo a specular reflection. This keeps fluids A and B separated, as if they were immiscible, and preserves a sharp interface with a fixed position without affecting the flow.

4.2. Periodic Poiseuille flow of two similar fluids

To show that the specular reflections at the interface have no effect on the flow we performed the periodic Poiseuille flow simulation, described in Section 4.1, with two fluids of type A. Since the two fluids are similar we can define a single friction factor ($\gamma = 9.0$) for all type of interactions, as if the system contains a single phase. To proof that our system is in the regime where the Navier–Stokes equations are valid we doubled the system size in the x-direction to $L_x = 16$, divided the body force by four and repeated the periodic Poiseuille flow simulation with two fluids of type A. The resulting stationary velocity profiles are plotted in Fig. 2 together with the analytic solution given by Eq. (8). The measurement error is within 1% of $V_z^{\max}$, which is about the size of the symbols. Clearly, there is no effect of system size, since both simulated profiles are on top of the analytic solution. This is also observed when the two fluids are of type B. Thus, we may conclude that the system we study is correctly described by the Navier–Stokes equations. The smooth profile at the interfaces indicates that the specular reflections do not affect the flow.

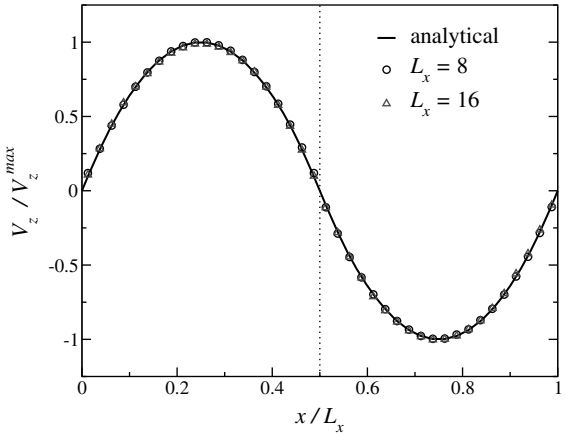

Fig. 2. Velocity profiles for stationary periodic Poiseuille flow of two similar immiscible fluids. The dotted line marks the position of the interface in the middle of the system.

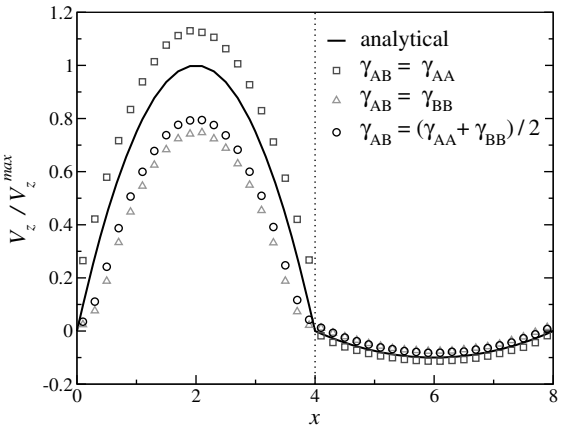

Fig. 3. Velocity profiles obtained with different γ_{AB}-values for stationary periodic Poiseuille flow of two dissimilar immiscible fluids.

4.3. Periodic Poiseuille flow of two dissimilar fluids

The friction a DPD particle exerts on another particle has a microscopic background and, therefore, depends on the type of fluid a particle represents. In a two-phase system of fluid A and B the specific friction between particles of fluid A is denoted by γ_{AA}, and between fluid B particles by γ_{BB}. When it is assumed that no additional chemical interaction exists between fluid A and B, the correct friction factor between A and B particles is expected to have a value in-between γ_{AA} and γ_{BB}. To explore the effect of the unlike friction factor γ_{AB} we consider two extreme cases: (1) the friction between unlike particles is set equal to the friction between particles of the less viscous fluid A, $\gamma_{AB} = \gamma_{AA}$, or (2) it is set equal to that of the more viscous fluid B, $\gamma_{AB} = \gamma_{BB}$. Thirdly, the arithmetic mean of these extremes is applied, $\gamma_{AB} = \frac{1}{2}(\gamma_{AA} + \gamma_{BB})$. All three cases are tested for the periodic Poiseuille flow problem described in Section 4.1.

The resulting stationary velocity profiles are plotted in Fig. 3 together with the analytical solution. Again, the measurement error is about the size of the symbols. First of all, the distinct difference between the profiles of the extreme cases shows that the flow field is indeed sensitive for changes in γ_{AB}. Evidently, the friction between the two adjacent fluids has an impact on the velocity distribution. Furthermore, none of the applied values for γ_{AB} produces the correct velocity profile. Deviations up to 25% of the analytical values are observed. Since interfacial tension, boundary and size effects are absent in the system studied, the friction factor between unlike fluids is responsible for these large deviations. This stresses the importance of the unlike friction factor and points out that accurate modelling of multi-viscosity systems relies on its correct value. The analytical velocity profile lies between those of the extreme cases. This proves that the correct unlike friction factor has indeed a value in-between the friction factors of the pure fluids. However, it is not simply given by the arithmetic mean.

5. The lever rule

A relation for the friction factor between two unlike fluids A and B can be found when we zoom in on the interaction across the interface between a particle i of fluid A and j of fluid B. Assume a correct flow field, so particles i and j are (on average) on the analytical velocity profile, as illustrated schematically in Fig. 4. Now, suppose that fluid B on the right of the interface is similar to fluid A, as if the systems contains a single phase. Then, the flow pattern around the interface will be symmetrical (see Fig. 2). In this hypothetical situation, the particle on the position of j is denoted by j^* and is, now, (on average) on the analytical velocity profile for this single phase situation, represented by the dashed line in Fig. 4. The interaction of particle i with particles j or j^* results both in the correct velocity of i. The strength of these interactions is, thus, equal. This is true when particles j and j^* exert the same drag force on particle i,

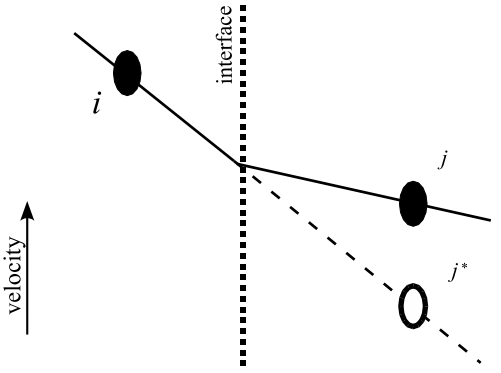

Fig. 4. Schematic drawing of particles interacting across the interface of two adjacent fluids. The particles are on the analytical velocity profile.

i.e. $\mathbf{F}_{ij}^{\mathrm{D}} = \mathbf{F}_{ij^*}^{\mathrm{D}}$. Using Eq. (2) this leads to the following expression for the friction factor between i of fluid A and j of fluid B:

$$\gamma_{ij} = \gamma_{ij^*} \cdot \frac{\mathbf{v}_{ij^*}}{\mathbf{v}_{ij}}. \tag{10}$$

Since $\gamma_{ij^*} = \gamma_{\mathrm{AA}}$, an input parameter, Eq. (10) gives a relation for the friction factor between unlike fluids that can be solved when $\mathbf{v}_{ij^*}$ and $\mathbf{v}_{ij}$ are known. If there exists an analytical solution for the velocity distribution in the system it is possible to calculate $\mathbf{v}_{ij^*}$ and $\mathbf{v}_{ij}$, and solve Eq. (10). This implies that under these circumstances we can define an unlike friction factor that produces the correct flow profile.

An analytical solution exists for the periodic Poiseuille flow problem described in Section 4.1 and is given by Eq. (8). Substituting this analytical solution for the velocity into Eq. (10) and using Eq. (7) we get

$$\gamma_{ij} = \gamma_{ii} \cdot \frac{h_i + h_j}{h_i + \frac{\mu_i}{\mu_j} \cdot h_j}, \tag{11}$$

where h is a function that depends on the position x of a particle in the fluid layer and the width W of that layer

$$h_i = x_i \cdot (x_i/W_i - 1). \tag{12}$$

When the dissipative forces are dominant, the kinetic contribution to the viscosity is negligible. Assuming this is true for fluids A and B, we can replace the viscosity terms in Eq. (11) by the dissipative part μ_{D} of Eq. (6) and derive the following relation for the friction factor between unlike fluids:

$$\gamma_{ij} = \frac{h_i + h_j}{h_i/\gamma_{ii} + h_j/\gamma_{jj}}. \tag{13}$$

Since $\gamma_{ij} = \gamma_{ji}$, Eq. (13) conserves the important pairwise additive character, $\mathbf{f}_{ij} = -\mathbf{f}_{ji}$, of the interparticle forces. Note that γ_{ij} goes to γ_{ii} for $h_j \to 0$ and to γ_{jj} for $h_i \to 0$, in fact, implying that the relation in Eq. (13) represents a kind of *lever rule* for the friction factor between unlike fluids. Such a γ_{ij}-lever rule can be derived, in similar ways, for other kind of flow situations, provided that a solution of the velocity distribution is available. When applied to all unlike interactions across the interface, the γ_{ij}-lever rule should lead to the desired shear stress between the different fluids and the correct flow profile.

To validate the lever rule of Eq. (13) simulations are performed using the same system as described in Section 4.1. Fig. 5 compares the stationary velocity profile obtained with the lever rule to the analytical solution. The profiles obtained for the extreme cases $\gamma_{\mathrm{AB}} = \gamma_{\mathrm{AA}}$ and $\gamma_{\mathrm{AB}} = \gamma_{\mathrm{BB}}$ are shown as well. The effect of the different γ_{AB}'s is very clear. For $\gamma_{\mathrm{AB}} = \gamma_{\mathrm{AA}}$ and $\gamma_{\mathrm{AB}} = \gamma_{\mathrm{BB}}$ the relative error in the simulated velocity is unacceptable, above 10% in a large part of the system. The velocity profile obtained with γ_{AB} from the lever rule of Eq. (13) shows, however, excellent agreement with the analytical solution.

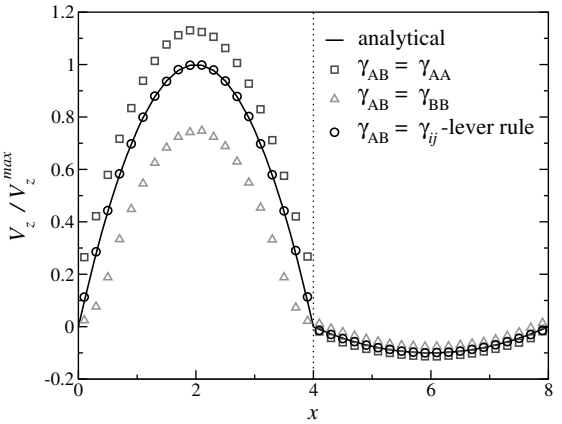

Fig. 5. Comparison of the analytical and simulated velocity profiles for stationary periodic Poiseuille flow of two immiscible fluids.

6. What if the solution of the flow profile is unknown?

The procedure described in Section 5 yields the true value of the unlike friction factor when viscosity is dominated by dissipative forces. However, it requires (a priori) a solution of the velocity profile. For some simple flow situations analytical solutions are available. Often the flow in multiphase systems is very complex, containing, for instance, irregular interfaces with a time-dependent shape and position. Then, the velocity distribution cannot be solved, which makes it impossible to derive a γ_{ij}-lever rule. Here, we present two methods for calculating the unlike friction factor when the solution of the flow profile is unknown. Both methods are tested under the same conditions as the γ_{ij}-lever rule in the periodic Poiseuille flow experiment described in Section 4.1.

6.1. Constant gradient method

When it is assumed that the velocity profile is linear near the interface, the shear stress left and right of the interface are equal and given by

$$-\left(\mu \cdot \frac{\mathrm{d}V_z}{\mathrm{d}x}\right)_{\text{left}} = -\left(\mu \cdot \frac{\mathrm{d}V_z}{\mathrm{d}x}\right)_{\text{right}}. \tag{14}$$

Then, the velocity difference $\mathbf{v}_{ij}$ between two interacting particles can be expressed in terms of the constant velocity gradient and the distance of these particles to the interface. With the help of Eq. (14) this approach makes it possible to solve Eq. (10) without knowing the exact analytical solution explicitly and is referred to as the *constant gradient* method. A relation similar to Eq. (13) is derived, only now $h_i = \Delta x_i$, where Δx is the absolute distance of a particle to the interface. This means that the unlike friction factor only depends on the distance of interacting particles to the interface. The interface in our periodic Poiseuille flow experiment has a fixed and predefined position, so it is not difficult to determine this distance. In most situations, however, the interface moves and is it necessary to determine its position in time with some kind of tracking technique. Fig. 6 shows that the stationary velocity profile obtained with the constant gradient method agrees well with the analytic solution and lever rule result.

6.2. Mean value method

The constant gradient method described in the previous section requires the position of the interface. In some special cases this position is known, but otherwise it must be tracked. Numerous tracking techniques are possible, varying in complexity and computational load. Nevertheless, pinpointing the exact location of the interface is difficult, especially for highly deformable and irregular interfaces in 3D-space. Besides, one

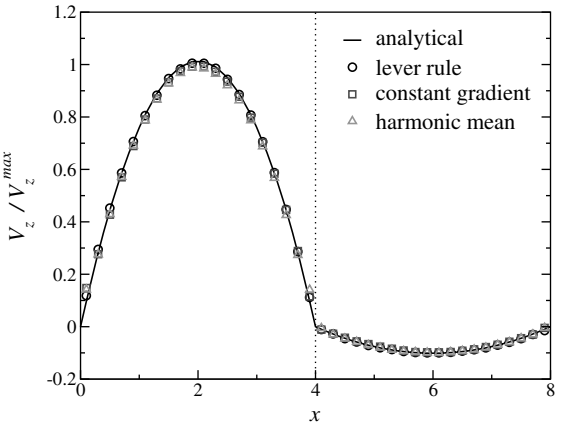

Fig. 6. Comparison of the analytical and simulated velocity profiles for stationary periodic Poiseuille flow of two immiscible fluids.

of the attractive features of DPD in the area of multiphase flow is its particle-based nature, meaning that phase behaviour arises from the interacting particles alone and the position of the interface is irrelevant. When the unlike friction factor is related to the position of the interface, however, this feature is lost. Then, the precision of localizing the exact position of the interface influences the reliability of the DPD model in simulating multiphase flows, a well-known drawback in continuum-based techniques. A relation for the unlike friction factor that depends only on the friction factors of the pure fluids rather than on the distance to the interface is, therefore, highly desirable.

As a first option in this respect one can calculate an average friction factor $\langle\gamma_{ij}\rangle$ with

$$\langle\gamma_{ij}\rangle = \frac{\int_0^{r_c}\int_{\Delta x_j - r_c}^{0}\gamma_{ij}\,\mathrm{d}\Delta x_i\,\mathrm{d}\Delta x_j}{\int_0^{r_c}\int_{\Delta x_j - r_c}^{0}\mathrm{d}\Delta x_i\,\mathrm{d}\Delta x_j}, \tag{15}$$

where γ_{ij} is the relation for the unlike friction factor that comes from the constant gradient method. This eliminates Δx_i and Δx_j, leading to a relation that only involves the friction factors of the pure fluids. A second option is suggested by the fact that the analytical velocity profile in Fig. 3 lies in-between the profiles of the extreme cases $\gamma_{AB} = \gamma_{AA}$ and $\gamma_{AB} = \gamma_{BB}$. It implies that a γ_{AB}-value, somewhere between these extremes, exists that leads to agreement with the true solution. This value is not the arithmetic mean of γ_{AA} and γ_{BB} as shown previously in Section 4.3, but may be an average of some other kind. The general relation for calculating a mean value between a friction factor γ_{ii} and γ_{jj} is given by

$$M_p = \left(\frac{1}{2}\left(\gamma_{ii}^p + \gamma_{jj}^p\right)\right)^{1/p}, \tag{16}$$

returning the arithmetic mean for power $p = 1$. Taking a closer look at Eq. (13) we see that it simplifies to the relation of the harmonic mean $p = -1$ when $h_i = h_j$ for all ij-interactions. Consequently, we may take this as a hint at the harmonic mean. We decided to test Eq. (16) for powers ranging from $p = -2$ to $p = 1$ in the periodic Poiseuille flow experiment. In addition, the average value $\langle\gamma_{ij}\rangle$ calculated with Eq. (15) is tested. The best agreement with the analytical solution is achieved when the unlike friction factor is given by the harmonic mean M_{-1}, which is in accordance with the form of the γ_{ij}-lever rule. Hence, the unlike friction factor of the mean value method is given by the harmonic mean from now on. The velocity profile obtained with the harmonic mean is also plotted in Fig. 6. Again, the comparison is good.

7. Validation of the methods

Three methods are derived to calculate the friction factor between unlike fluids in a two-phase system. All three methods are tested for the fully developed periodic Poiseuille flow of two adjacent immiscible fluids A and B. Both fluids are well within the collective dynamic regime and differ a factor 10 in viscosity. In this

section, we study the reliability of the methods at different dynamic regimes and viscosity ratios. In addition, the methods are employed and tested for instationary flows.

7.1. The dynamic regime

In Section 5, we derived the γ_{ij}-lever rule, a relation for the friction factor between particles of unlike fluids that is based on the analytical solution of the flow field and assuming that the viscosity scales linearly with the friction factor. This assumption is true when the kinetic contribution to the viscosity μ_K is negligible as compared to the dissipative contribution μ_D. The same assumption is applied in the constant gradient and mean value method presented in Section 6. According to Eq. (6), the kinetic contribution to the viscosity of the fluids used so far is 5.25% and 0.04% for fluid type A and B, respectively. Surprisingly, all three methods still work properly at this relatively high kinetic contribution for fluid type A. Here, we test to which extent our assumption is still valid, and the methods reliable, by varying the dynamic regime of the fluids in the system.

Simulations are performed with the periodic Poiseuille flow experiment described in Section 4.1 for six different two-phase systems. The temperature and friction factors of the two fluids in each system are given in Table 1. Going from left to right in the table the kinetic contribution to the viscosity increases. In all systems, the viscosity of fluid A and B is kept constant at a value of 3.63 and 36.3, respectively. Since the kinetic contribution to the viscosity of fluid B remains negligible (<0.2%), we focus on the dynamic regime of the less viscous fluid A expressed as the ratio μ_D/μ. The reliability of the γ_{ij}-lever rule, constant gradient and mean value method is validated by determining the root-mean-square (RMS) error of the simulated stationary velocity distribution in fluid A, defined as

$$\mathrm{RMS} = \sqrt{\frac{\sum^{N}(\Delta V_z/V_z^{\max})^2}{N}}, \tag{17}$$

where N is the number of slabs left of the interface and ΔV_z the deviation of the simulated velocity from the analytical solution in a slab. Fig. 7 shows that the RMS error increases (exponentially) for all three methods when the ratio μ_D/μ decreases and kinetic forces become more dominant. This trend was to be expected, while

Table 1
Parameter setting of six two-phase systems

k_BT	0.5	1.0	1.5	2.0	2.0	1.0
γ_{AA}	9.00	8.00	6.45	4.45	2.96	1.00
γ_{BB}	109.20	108.05	106.80	106.09	106.09	108.05

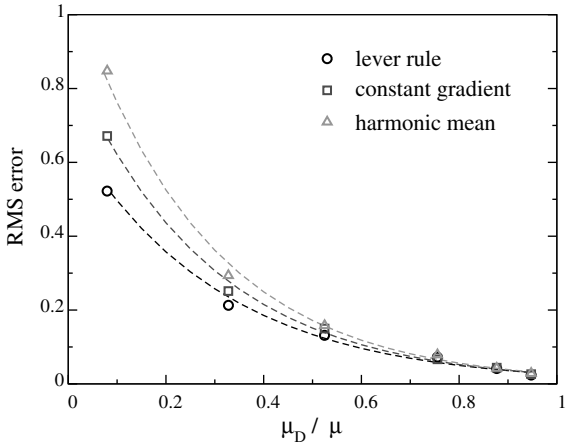

Fig. 7. Performance of the lever rule, constant gradient and mean value method at different dynamic regimes. The measurement errors are of the size of the symbols and the dashed lines are exponential fits of the simple form $y = y_0 \cdot e^{ax}$.

the assumption that the viscosity scales linearly with the friction factor becomes less valid. Now, the dynamic regime at which the applied methods can be considered reliable depends on the error one is willing to accept. When accepting an error in the velocity equal to 5% of $V_z^{\max}$, the methods remain applicable down to $\mu_D/\mu = 0.85$ according Fig. 7, which corresponds to a kinetic contribution to the viscosity of less than 15%. Apparently, the methods are only useful in a small range of dynamic regimes. It corresponds, however, to the typical conditions used in most simulations as noted before [16].

7.2. The viscosity ratio

The viscosity ratio μ_B/μ_A of the fluids A and B used so far is 10. Here, we investigate if the performance of the three methods introduced depends on this ratio. To this end, periodic Poiseuille flow simulations are performed at viscosity ratios ranging from 2 to 100. The viscosity ratio is varied by changing the viscosity of fluid B, using the input parameter γ_{BB}. The simulation results are, again, evaluated in terms of the RMS error of the velocity distribution in fluid A, given by Eq. (17). No significant increase of the RMS error is observed. Apparently, the performance of the methods is not influenced by the viscosity ratio between the fluids.

7.3. Time-dependent flow

In this section, the performance of the γ_{ij}-lever rule, constant gradient and mean value method is studied for time-dependent flow. We model the development of the velocity profile for periodic Poiseuille flow of two adjacent immiscible fluids that are initially at rest. The velocity distribution for unsteady Poiseuille flow of a single fluid can be solved theoretically [18] and is given in dimensionless form by

$$\phi = 1 - \xi^2 - \frac{32}{\pi^3}\sum_{q=0}^{\infty}\frac{(-1)^q}{(2q+1)^3}\cos\left[\frac{(2q+1)\pi\xi}{2}\right]\exp\left[\frac{-(2q+1)^2\pi^2\tau}{4}\right], \tag{18}$$

where $\tau = 4\nu\cdot t/W^2$ with ν the kinematic viscosity. Our two-phase flow problem transforms into two single phase situations when the velocity on the interface remains zero, and allows us to use Eq. (18) as a bench mark, here. If we consider two adjacent layers of fluid A and B, the velocity on the interface stays zero if the net force on fluid A and B counterbalance one another at all times. This condition can only be met when the dimensionless time τ is equal for the flow in both fluid layers and adds an extra term to Eq. (7) to give

$$-\frac{\mathbf{f}_A^b}{\mathbf{f}_B^b} = \frac{W_B}{W_A} = \sqrt{\frac{\nu_B}{\nu_A}}, \tag{19}$$

where the variables in the two adjacent fluid layers are denoted by a subscript.

The unsteady two-phase flow simulations are performed in a large rectangular box of sizes $12\times 40\times 25$ with a system of $n = 10$, $k_BT = 0.5$, $\gamma_{AA} = 9.0$ and $\gamma_{BB} = 42.0$. This parameter setting results in a viscosity ratio $\nu_B/\nu_A = 4$ between the fluids. To maintain a zero velocity on the interface the width of fluid layer B should be twice the width of layer A according Eq. (19), which is the case when $W_A = 4.0$ and $W_B = 8.0$. The body force $\mathbf{f}_A^b$, acting on fluid A and pointing in the z-direction, is set to 9.075×10^{-2} so that $V_z^{\max} = 0.5$ according Eq. (8). The body force $\mathbf{f}_B^b$ acting on fluid B follows from Eq. (19). Although the theoretical solution of the velocity is known for the time-dependent flow process, we employ the γ_{ij}-lever rule derived for the stationary situation. While the solution of the stationary flow profile is given by Eq. (8), the lever rule is, again, given by Eq. (13). In Fig. 8, the instationary velocity profiles obtained with the γ_{ij}-lever rule, constant gradient and mean value method are compared with the theoretical solution at three points in time. The simulated profiles are obtained by measuring the instantaneous velocity in the 40 slabs dividing the system. For clarity reasons, we plotted, however, only half of the data points. The error in the velocity measurements is reduced to the size of the symbols used in Fig. 8 by averaging over 10 simulation runs. The agreement with theory is again very good for all three methods, which proves their validity for instationary situations.

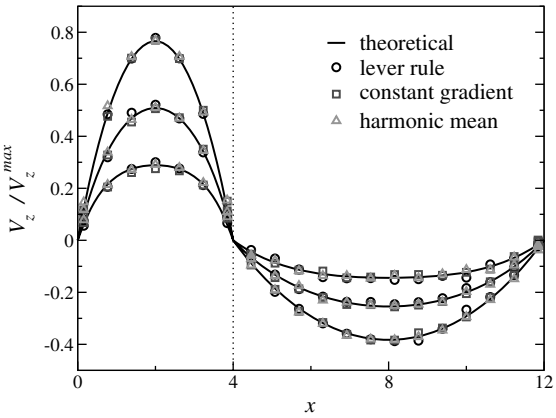

Fig. 8. Development of the velocity profile for periodic Poiseuille flow of two immiscible fluids at time $\tau = 0.15$, 0.30 and 0.60.

8. Real interfaces

In our simulations thus far all particles have the same affinity with each other, regardless of their type. The adjacent fluids in the two-viscosity test cases are, therefore, miscible and have to be kept separated artificially by means of specular reflections in the interface. The reason to do so is to avoid interfacial effects so that we can easily identify the effects related to the unlike friction factor and compare our results to theory. In the previous sections, we studied these effects and established three methods to define a suitable value for the unlike friction factor: the lever rule, the constant gradient and mean value method. Here, we like to test these three multi-viscosity methods in a more realistic situation with interfacial tension. This is done by increasing the repulsion between the unlike fluids so that a (real) self-supporting interface will evolve. Depending on its strength, a positive interfacial tension will lead to depletion of particles at the interface [7,20], and we expect a certain influence on fluid dynamics.

To validate the three methods in the context of the natural interface that is now created, we simulate the fully developed periodic Poiseuille flow of two adjacent fluids A and B. All settings are identical to those in Section 4.1 with the one exception that the repulsion between unlike particles at the interface is now twice the normal bulk repulsion, $a_{AB} = 2a$. This difference in repulsion between like and unlike particles results in an interfacial tension of 5.90 ± 0.05, as determined from the pressure tensor [20], which keeps the fluids separated. To maintain a straight interface located in the middle of the simulation box a specular reflection prevents the particles from diffusing across. Only few particles are subject to these moves; about 5% of the particles within the interaction radius of the interface per unit of time.

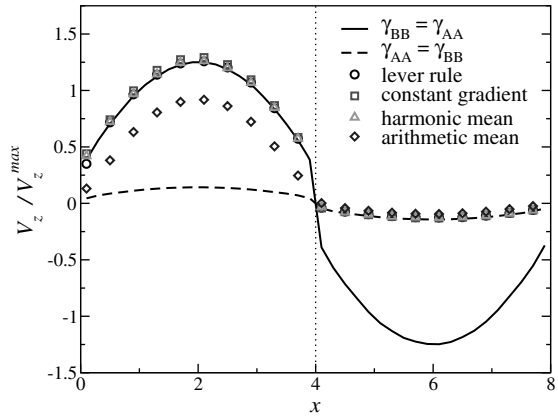

Fig. 9. Velocity profiles obtained for stationary periodic Poiseuille flow of two immiscible fluids separated by a real interface.

The stationary velocity profiles obtained with the three methods are plotted in Fig. 9. An analytical solution is unavailable for this more complex (mesoscopic) situation with interfacial tension. Therefore, we compare the results of our two-viscosity simulations to those where the fluids have the viscosity of fluid A or B, respectively. The flow pattern in fluid A should correspond to the case where both fluids have the viscosity of fluid A; $\gamma_{BB} = \gamma_{AA}$. In fluid B the flow pattern should correspond to the case where both fluids have the viscosity of fluid B; $\gamma_{AA} = \gamma_{BB}$. The velocity slip at the interface shows clearly the effect of interfacial tension on the flow. Note that this slip is exactly identical to that of the single-viscosity situations. Therefore, they must be interpreted as real interfacial effects that should not be ascribed to the methods we propose here. The results of the three methods agree well with those of the single-viscosity cases. The same agreement is observed in simulations with a more moderate interfacial tension. It proves that the methods derived for the ideal situation sketched in Section 4.1 are applicable to real interfaces as well. For comparison, the profile obtained with an unlike friction factor given by the arithmetic mean is plotted. Again, the arithmetic mean shows a large deviation.

9. Discussion

The fluids in our simulations are kept strictly separated by means of a specular reflection in the interface. In reality interfaces are permeable and particles are free to diffuse across. Interfacial forces, resulting from the repulsive particle-particle interactions, oppose this motion. At a high interfacial tension, as in Section 8 for instance, the diffusion of particles across the interface is unlikely to occur. The number of particles that cross the interface is small and will have little or no effect on the performance of the three multi-viscosity methods described. However, this number will increase when the interfacial tension becomes weaker, making the interface diffuse and fluids impure, until the fluids are perfectly mixed. If, and how, this affects the performance of the methods is at present unclear and subject to further investigation.

In the mesoscopic simulation technique applied here the viscosity is controlled by the dissipative forces between the fluid particles. Several particle-based techniques exist that use similar or related forces. A good example is the alternative approach to DPD introduced by Lowe [21]. In this technique, the pairwise stochastic and dissipative interactions are replaced by pairwise thermal bath collisions, relaxing the system to equilibrium. These bath collisions occur with a certain probability Γ, a quantity of the same physical meaning as the friction factor γ in DPD. It is important to note that the relation of Γ and γ with viscosity is similar. It implies that the multi-viscosity methods described will also be applicable to this alternative DPD model, simply by replacing γ with Γ. Thus, the three methods introduced here for DPD can be useful in other techniques as well.

10. Conclusion

In this paper, we aim at modelling multiple viscosities in a single DPD system. To this end a system with two fluids of different viscosity is studied. This two-viscosity test case requires the definition of three friction factors. Two for the interactions between identical particles, directly related to the fluid's viscosity, and one for the interaction between unlike particles. We demonstrated that accurate modelling of such a multi-viscosity system strongly depends on this last, unlike friction factor.

Three methods are presented here to define the unlike friction factor. The first method is based on the analytical solution of the fully developed velocity profile and yields a kind of lever rule. Excellent agreement is found between analytical and simulated velocity profiles when this lever rule is employed for stationary periodic Poiseuille flow of adjacent immiscible fluids. An undesirable aspect of the lever rule is that it requires the analytical solution, meaning it is of limited use in practice. A good alternative in this respect is the constant gradient method that gives a relation for the friction factor by assuming a linear velocity profile near the interface. A drawback of this second method is, however, that it requires the position of the interface. The third method calculates the unlike friction factor from the harmonic mean of the friction factors of the pure fluids and is, thus, independent of the whereabouts of the interface. This method is, therefore, readily applicable to complex multiphase flows.

Since the methods are derived for the dynamic regime where dissipative forces dominate, one should check the reliability when this condition is violated. We found that all three methods produce acceptable results in

the collective dynamic regime $\mu_D/\mu \geqslant 0.85$. Furthermore, the methods stay reliable at high viscosity differences and appeared to work just as well for time-dependent as stationary flow. As a final test, the methods are applied to a system containing an interface with interfacial tension. Although this alters the dynamic properties at the interface and affects the flow considerably, all three methods yield the correct velocity distribution. This proves that the methods introduced give an appropriate value for the unlike friction factor and make reliable modelling of multi-viscosity systems with DPD possible.

Acknowledgements

As part of the OSPT Research Program *Computational fluid dynamics of disperse multiphase flows* this work is supported financially by AKZO Nobel Chemical Research, DSM Research and Shell Global Solutions International B.V.

References

[1] P.J. Hoogerbrugge, J.M.V.A. Koelman, Simulating microscopic hydrodynamics phenomena with dissipative particle dynamics, Europhys. Lett. 19 (1992) 155–160.
[2] J.M.V.A. Koelman, P.J. Hoogerbrugge, Dynamic simulation of hard-sphere suspensions under steady shear, Europhys. Lett. 21 (1993) 363–368.
[3] A.G. Schlijper, P.J. Hoogerbrugge, C.W. Manke, Computer simulation of dilute polymer solutions with the dissipative particle dynamics method, J. Rheol. 39 (1995) 567–579.
[4] S.M. Willemsen, H.C.J. Hoefsloot, P.D. Iedema, Mesoscopic simulation of polymers in fluid dynamics problems, J. Stat. Phys. 107 (2002) 53–65.
[5] S. Chen, N. Phan-Thien, X.J. Fan, B.C. Khoo, Dissipative particle dynamics simulation of polymer drops in a periodic shear flow, J. Non-Newton. Fluid Mech. 118 (2004) 65–81.
[6] K.E. Novik, P.V. Coveney, Using dissipative particle dynamics to model binary immiscible fluids, Int. J. Mod. Phys. C 8 (1997) 909–918.
[7] R.D. Groot, P.B. Warren, Dissipative particle dynamics: bridging the gap between atomistic and mesoscopic simulation, J. Chem. Phys. 107 (1997) 4423–4435.
[8] A.T. Clark, M. Lal, J.N. Ruddock, P.B. Warren, Mesoscopic simulation of drops in gravitational and shear fields, Langmuir 16 (2000) 6342–6350.
[9] M. Kranenburg, M. Venturoli, B. Smit, Phase behavior and induced interdigitation in bilayers studied with dissipative particle dynamics, J. Phys. Chem. 107 (2003) 11491–11501.
[10] P. Español, P.B. Warren, Statistical mechanics of dissipative particle dynamics, Europhys. Lett. 30 (1995) 191–196.
[11] C.A. Marsh, G. Backx, M.H. Ernst, Fokker–Planck–Boltzmann equation for dissipative particle dynamics, Europhys. Lett. 38 (1997) 411–415.
[12] I. Pagonabarraga, M.H.J. Hagen, D. Frenkel, Self-consistent dissipative particle dynamics algorithm, Europhys. Lett. 42 (1998) 377–382.
[13] A.J. Masters, P.B. Warren, Kinetic theory for dissipative particle dynamics: the importance of collisions, Europhys. Lett. 48 (1999) 1–7.
[14] S.M. Willemsen, H.C.J. Hoefsloot, P.D. Iedema, No-slip boundary condition in dissipative particle dynamics, Int. J. Mod. Phys. C 11 (2000) 881–890.
[15] P. Español, M. Serrano, Dynamical regimes in the dissipative particle dynamics model, Phys. Rev. E 59 (1999) 6340–6347.
[16] M. Ripoll, M.H. Ernst, P. Español, Large scale and mesoscopic hydrodynamics for dissipative particle dynamics, J. Chem. Phys. 115 (2001) 7271–7284.
[17] J.A. Backer, C.P. Lowe, H.C.J. Hoefsloot, P.D. Iedema, Poiseuille flow to measure the viscosity of particle model fluids, J. Chem. Phys. 122 (2005) 154503.
[18] R.B. Bird, W.E. Stewart, E.N. Lightfoot, Transport Phenomena, Wiley, New York, 1960.
[19] C.A. Marsh, J.M. Yeomans, Dissipative particle dynamics: the equilibrium for finite time steps, Europhys. Lett. 37 (1997) 511–516.
[20] D. Frenkel, B. Smit, Understanding Molecular Simulation: From Algorithms to Applications, second ed., Academic Press, San Diego, 2002.
[21] C.P. Lowe, An alternative approach to dissipative particle dynamics, Europhys. Lett. 47 (1999) 145–151.